Impact of Dust Source Patchiness on the Existence of a Constant Dust Flux Layer During Aeolian Erosion Events

S. Dupont, M. Klose, M R Irvine, C González-flórez, A. Alastuey, Jean-Marc Bonnefond, P Dagsson-waldhauserova, A Gonzalez-romero, T. Hussein, Eric Lamaud, et al.

JGR Atmospheres

RESEARCH ARTICLE
10.1029/2023JD040657

Impact of Dust Source Patchiness on the Existence of a Constant Dust Flux Layer During Aeolian Erosion Events

S. Dupont[1], M. Klose[2], M. R. Irvine[1], C. González-Flórez[3,4], A. Alastuey[5], J.-M. Bonnefond[1], P. Dagsson-Waldhauserova[6,7], A. Gonzalez-Romero[3,4,5], T. Hussein[8,9], E. Lamaud[1], H. Meyer[2], A. Panta[10], X. Querol[5], K. Schepanski[11], S. Vergara Palacio[2], A. Wieser[2], J. Yus-Díez[5,12,13], K. Kandler[10], and C. Pérez García-Pando[3,14]

[1]INRAE, Bordeaux Sciences Agro, ISPA, Villenave d'Ornon, France, [2]Institute of Meteorology and Climate Research—Department Troposphere Research (IMK TRO), Karlsruhe Institute of Technology (KIT), Karlsruhe, Germany, [3]Barcelona Supercomputing Center (BSC), Barcelona, Spain, [4]Department of Civil and Environmental Engineering, Polytechnical University of Catalonia (UPC), Barcelona, Spain, [5]Institute of Environmental Assessment and Water Research (IDAEA-CSIC), Barcelona, Spain, [6]Agricultural University of Iceland, Reykjavik, Iceland, [7]Agricultural University of Iceland, Iceland—Czech University of Life Sciences Prague, Hvanneyri, Iceland, [8]Department of Physics, Environmental and Atmospheric Research Laboratory (EARL), University of Jordan, School of Science, Amman, Jordan, [9]Faculty of Science, University of Helsinki, Institute for Atmospheric and Earth System Research (INAR), Helsinki, Finland, [10]Institute of Applied Geosciences, Technical University Darmstadt, Darmstadt, Germany, [11]Institute of Meteorology, Freie Universität Berlin, Berlin, Germany, [12]Grup de Meteorologia, Departament de Física Aplicada, Universitat de Barcelona, Barcelona, Spain, [13]Now at Center for Atmospheric Research, University of Nova Gorica, Ajdovščina, Slovenia, [14]ICREA, Catalan Institution for Research and Advanced Studies, Barcelona, Spain

Key Points:

- Size-resolved dust emission fluxes have been estimated for the first time at different heights during erosion events in Iceland and Jordan
- Unlike in Jordan, the absence of a constant dust flux layer in Iceland is due to the dust source patchiness related to surface humidity
- Our results highlight the importance of estimating dust fluxes above a dust blending height that depends on the dust source patchiness

Supporting Information:

Supporting Information may be found in the online version of this article.

Correspondence to:

S. Dupont,
sylvain.dupont@inrae.fr

Citation:

Dupont, S., Klose, M., Irvine, M. R., González-Flórez, C., Alastuey, A., Bonnefond, J.-M., et al. (2024). Impact of dust source patchiness on the existence of a constant dust flux layer during Aeolian erosion events. *Journal of Geophysical Research: Atmospheres*, *129*, e2023JD040657. https://doi.org/10.1029/2023JD040657

Received 21 DEC 2023
Accepted 4 MAY 2024

Abstract Dust emission fluxes during wind soil erosion are usually estimated using a dust concentration vertical gradient, by assuming a constant dust flux layer between the surface and the dust measurement levels. Here, we investigate the existence of this layer during erosion events recorded in Iceland and Jordan. Size-resolved dust fluxes were estimated at three levels between 2 and 4 m using the eddy-covariance method. Dust fluxes were found mainly constant only between the two upper levels in Iceland, the lower dust flux being often stronger and richer in coarse particles, while dust fluxes in Jordan were nearly constant across all levels. The wind dynamics could not explain the absence of a constant dust flux layer in Iceland. We show that the presence of stationary dust source patches in Iceland, related to surface humidity, created a non-uniform dust layer near the surface, named dust roughness sublayer (DRSL), where individual plumes behind each patch interact but do not fully mix. The lowest dust measurement level was probably located within this sublayer while the upper ones were located above, such that there the emitted dust became spatially well-mixed. This explains near the surface in Iceland, the more intermittent dust concentration, its low correlation with the dust concentrations above, and the richer dust flux in coarse particles due to their lower deposition contribution. Our findings highlight the importance of estimating dust fluxes above a dust blending height whose characteristics depend on the dust source patchiness caused by surface humidity or the presence of sparse non-erosive elements.

Plain Language Summary During soil erosion by wind, dust flux from the surface is estimated at a few meters height, by assuming the existence of a constant dust flux layer between the surface and the dust measurement levels. Here, we investigated for the first time the existence of this layer during erosion events in Iceland and Jordan, by estimating the dust fluxes at three levels between 2 and 4 m height. In Iceland, the dust fluxes were constant only between the two upper levels. In Jordan, the dust fluxes remained constant across all levels. We demonstrates that the absence of a constant dust flux layer in Iceland is due to patches of stationary dust sources, which are related to surface humidity. These patches created a non-uniform dust layer near the surface, known as the dust roughness sublayer. In this layer, individual plumes behind each patch interact but do not fully mix. The lowest dust measurement level was likely within this sublayer, while the upper measurements were located above it. Our findings highlight the importance of estimating dust fluxes above a dust blending height, which depends on the patchiness of the dust source caused by surface humidity or the presence of sparse non-erosive elements.

1. Introduction

The hypothesis of a constant dust flux layer above erodible surfaces is systematically considered when estimating dust emission fluxes from field measurements (e.g., Dupont et al., 2021; Gillette et al., 1972). The dust flux comprises the diffusive and gravitational settling fluxes. The latter flux is only significant for particles larger than approximately 10 μm (Fratini et al., 2007). The constant dust flux layer hypothesis is used when relating the estimated dust flux at several meters height to the flux at the surface, including emission and deposition fluxes. This hypothesis is used also when the Monin-Obukhov similarity theory (MOST, Monin & Obukhov, 1954) is applied to estimate the diffusive flux from the vertical gradient of dust concentration, assuming horizontal homogeneity (no horizontal advection) and stationarity (no time variation). However, the existence of a constant dust flux layer has not yet been verified.

In the atmospheric surface layer, which is the layer near the surface (smaller than about 100 m depth) where wind shear dominates the production of turbulence over buoyancy and where MOST is applicable, momentum and scalar fluxes (heat, water vapor, gas, particles) are not expected to be strictly constant. This is because the vertical profiles of these fluxes result from the contribution of both the surface fluxes and the entrainment fluxes at the top of the atmospheric boundary layer (Tennekes, 1973; Wyngaard & Brost, 1984). However, above a homogeneous surface and for well-developed atmospheric boundary layer with a depth of about 1 km, the near-surface atmospheric layer (<10 m depth) can be well approximated as a constant flux layer with flux variations within 1% of their surface values (Wyngaard, 1990). The absence of a near-surface constant flux layer would most likely be explained by flow unstationarity or surface inhomogeneity inducing horizontal advection.

The goal of this study is to test the existence of a constant dust flux layer close to the surface during daytime erosion events recorded above two erosive surfaces from two very different desert regions, one at a high-latitude location in Iceland and the other at a low-latitude location in Jordan. The Iceland campaign was co-organized by two projects: FRAGMENT (FRontiers in dust minerAloGical coMposition and its Effects upoN climaTe) and HiLDA (Iceland as a model for high-latitude dust sources—a combined experimental and modeling approach for characterization of dust emission and transport processes); and the Jordan campaign (J-WADI: Jordan Wind erosion And Dust Investigation) was co-organized by the FRAGMENT and Helmholtz Young Investigator Group "A big unknown in the climate impact of atmospheric aerosol: Mineral soil dust" projects. At both sites, a similar setup was deployed to estimate at three heights the diffusive fluxes of dust particles with diameters between 0.2 and 10 μm. For these small particle sizes, the gravitational settling flux is expected to be negligible compared to the diffusive flux.

To our knowledge, this is the first investigation of the existence of a constant dust flux layer from measurements. This absence of verification is explained by (a) the limited number of optical particle counters (OPC) deployed in field experiments to measure size-resolved dust concentration, mostly two OPCs (e.g., González-Flórez et al., 2023), and (b) the common use of the flux-gradient (FG) method to estimate the dust flux, which requires measuring concentration at two levels to estimate the dust flux between the two levels. Recently, in the continuity of Fratini et al. (2007) work, Dupont et al. (2021) developed an eddy-covariance (EC) approach to estimate the near-surface dust flux using only one OPC together with high frequency 3D wind measurements, where the flux is derived from the correlation between the dust concentration fluctuations and the vertical velocity fluctuations. The EC approach opens new perspectives to more easily obtain a vertical profile of the dust flux from a limited number of OPCs. This EC approach has been evaluated on soil erosion in Tunisia (Dupont, 2020, 2022; Dupont et al., 2019, 2021). During the campaigns in Iceland and Jordan, three OPCs were deployed between 2 and 4 m above the ground, paired with high-frequency sonic anemometers to estimate the EC dust flux at three heights, allowing the evaluation of the constant dust flux layer.

2. Materials and Methods

2.1. Experimental Sites

The Iceland campaign took place in the Vatnajökull National Park, from 10 August to 5 September 2021. The site was located in a terminal lake connected to a nearby glacier (N 64°54'55", W 16°46'35", 710 m a.s.l., see Figure 1a). This lake is mostly dry at that time of the year, with surface exposed to wind erosion. However, from 24 to 27 August, due to unusually high temperatures, the site was regularly flooded during the afternoon, resulting in deposition of fresh sediment from the glacier streams. The water quickly drained away and evaporated the

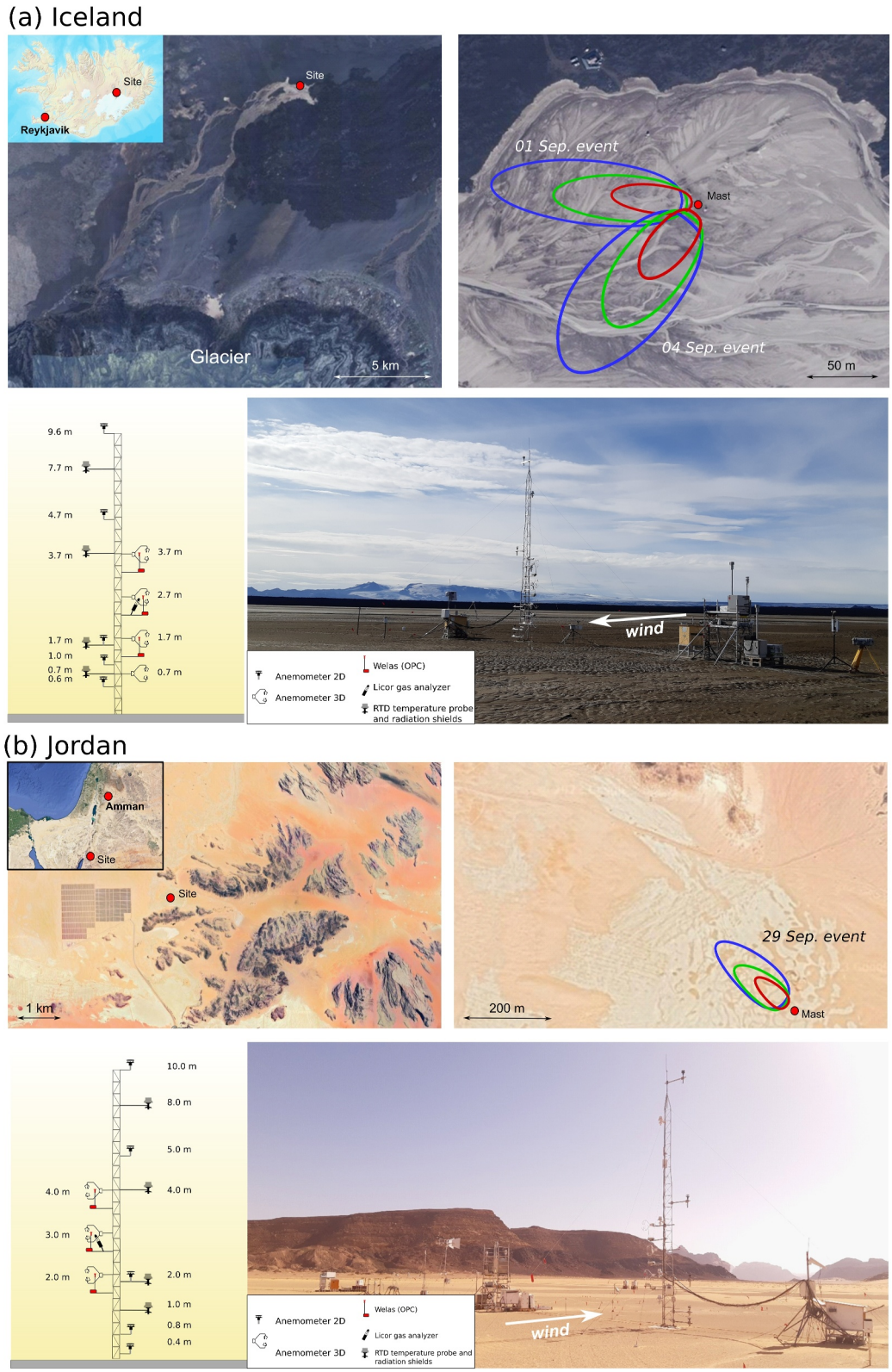

Figure 1. Iceland (a) and Jordan (b) experimental sites, including for each site: the localization of the site with its 10 m high mast (red dot); the 60%-flux footprints of the main erosion events at 1.7–2 m (red), 2.7–3 m (green) and 3.7–4 m (blue) high; a schematic description of the mast and sensors mounted on it; and a picture of the plot and mast. Satellite views are from the National Land Survey of Iceland and from Google Maps for Jordan. Flux footprints were estimated according to Kljun et al. (2015).

following morning, exposing the surface to wind erosion. The site was flat and devoid of substantial roughness elements (the roughness length is about 10^{-4} m as deduced from the mean wind velocity profile), with a long fetch (>500 m) for south and southwest winds, and a shorter fetch (about 150 m) for west winds due to the presence of a lava field, which also acted as a source of dust but in a distinct manner.

The J-WADI campaign took place in the north of the Wadi Rum desert in Jordan, from 9 September to 5 October 2022. The site was located between two gentle hills in the North and South (N 29°44'21", E 35°22'56", 790 m a.s.l., see Figure 1b), with a wind channeling mostly between them. The site between these two hills was flat without significant roughness elements (the roughness length is about 10^{-4} m), with a long fetch (>500 m) in the main wind direction (northwest).

2.2. Measurements

In both campaigns, a 10 m-high mast (Figures 1a and 1b) was equipped with 3D sonic anemometers (Campbell® Scientific CSAT3 at 0.7, 1.7, 2.7 and 3.7 m AGL in Iceland and at 2.0, 3.0 and 4.0 m AGL in Jordan) to measure wind velocity and air temperature fluctuations at 50 Hz. On the same mast, five 2D sonic anemometers and four aspirated shield temperature sensors were also installed but not used for the purpose of this study. These measurements were complemented by a temperature and relative humidity probe (Campbell Scientific HC2A-S3) mounted nearby the mast at 0.5 m AGL sampling at 0.5 Hz. A gas analyzer (LI-COR) was installed on the mast at 2.7 m AGL in Iceland and 3 m AGL in Jordan, close to the sonic anemometer, to measure water vapor (H_2O) and carbon dioxide (CO_2) turbulent fluctuations at 10 Hz, and to deduce their vertical fluxes using the EC approach by correlating H_2O and CO_2 fluctuations with the vertical wind velocity fluctuations. In the vicinity of the mast, a four-component net radiometer (Campbell Scientific NR01-L radiometer) was also installed at 1.5 m AGL to measure short-wave and long-wave upwelling and downwelling radiative fluxes.

Three OPCs (PALAS, PROMO 2000 equipped with the aerosol sensor WELAS 2300 system) were installed at 1.7, 2.7 and 3.7 m AGL in Iceland and at 2, 3 and 4 m AGL in Jordan to measure airborne dust concentration per size class at 1 Hz. These three OPCs were co-located with the sonic anemometers at the same heights in order to estimate the size-resolved vertical dust fluxes using the EC approach at the three heights. The three OPCs covered a 0.2–10-μm diameter range particles, with 32 intervals per decade. The OPCs determined the size and number of particles in sampled air in the optical chamber, delivered by a pump with a flow rate of 5 L min^{-1}, assuming spherical particles. The three OPCs were equipped with the same small sampling heads as in Dupont et al. (2021). These sampling heads were designed in order (a) to minimize disruption of the air near the sonic anemometers while sampling dust particles within the air, and (b) to minimize the time-lag between wind and dust measurements.

2.3. Dust Concentration Correction

At the end of the Iceland experiment, on 05 October 2021, the three OPCs were installed at equal height for intercomparison. A significant erosion event occurred during that day. The 1-min averaged dust concentrations per size bin from each OPC were compared against the averaged concentration of the three OPCs (see Figure S1 in Supporting Information S1). This allowed to estimate a multiplying correction factor for the concentration per size bin of each OPC relative to the average concentration of the three OPCs, in order to minimize the systematic differences in dust concentration measurements among OPCs (Figure 2a). A perfect match between OPCs would lead to a correction factor equal to one. Overall, the correction remained relatively small regardless of the particle size, between 0.85 and 1.25, and it was achieved with a good coefficient of determination ($R^2 > 0.85$) from 0.2 to 10 μm (Figure 2b).

Similarly, at the end of the Jordan campaign, from 02 to 05 October 2022, the three OPCs were installed at the same height for intercomparison. Unfortunately, no significant dust event occurred during that period, which limited the accuracy of the intercomparison, particularly for the finest (<0.4 μm) and coarsest (>7 μm) particles (see Figure S2 in Supporting Information S1). For these particle size ranges, the coefficient of determination (R^2) was less than 0.5 (Figure 2b). Nonetheless, the correction remained relatively small, between 0.85 and 1.10, with the exception of one OPC for fine particles (Figure 2a).

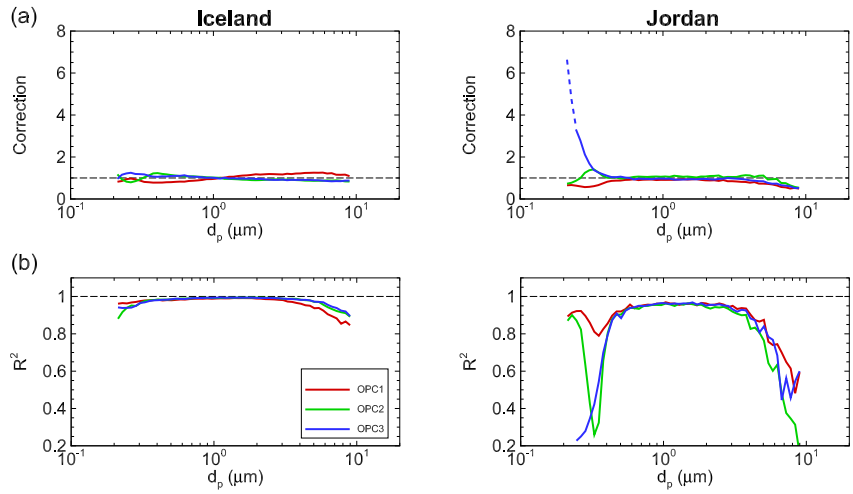

Figure 2. (a) Multiplying correction factor applied on the dust concentrations as deduced from the intercomparison of the three OPCs. The dashed curve for OPC3 of the Jordan event corresponds to an extrapolation due to the lack of fine dust particles for estimating accurately a correction. (b) Coefficient of determination (R^2) obtained from the intercomparison exercise. The horizontal black dashed lines indicate the perfect match values between OPCs: a multiplying correction factor and a coefficient of determination both equal to one. See Section 2.3 for further details.

In addition to correcting for differences in dust concentration measurements between OPCs, a correction due to the small sampling head used by the OPCs has to be applied as this sampling head underestimated the dust concentration with increasing particle size (Dupont et al., 2021). Here, we simply applied the correction estimated by Dupont et al. (2021) (their Figure 3a) through an intercomparison between similar OPCs, one with the small sampling head and two with the standard Total Suspended Particles (TSP) sampling head (BGI by Mesa Labs, Butler, NJ USA), which is commonly used in air quality measurements.

2.4. Selected Erosion Events

For this study, we focus only on the main erosion events of both campaigns, which occurred on 31 August, 01, 03 and 04 September for the Iceland campaign and 29 September for the Jordan campaign. In Iceland, these events happened a few days after the flooding period mentioned previously. This flooding deposited 30 cm of sediment, causing the surface to shift upwards. This explains that all instruments used during the chosen Iceland events were 30 cm lower than they were at the start of the experiment and lower than the instruments in Jordan.

For the sake of brevity, the Icelandic results are presented in this main document for only two reference events, those occurred on 01 and 04 September, which were characterized by different wind directions. Results from the events that occurred on 31 August and 03 September are presented in the Supplementary Material, as their behavior is similar to that on 01 September.

The main meteorological characteristics of the reference erosion events are presented in Table 1 and Figure 3 (Figure S3 in Supporting Information S1 for the 31 August and 03 September events). All erosion events took place during the day and lasted for several hours. Wind directions remained relatively constant during the events. All events in Iceland were characterized by westerly winds except for the 04 September event, which had a southwesterly wind (Figure 3a and Table 1). The Jordan event was characterized by a northwesterly wind. The Iceland events have notably stronger winds, with a mean surface friction velocity u_{*0} ranging between 0.32 and 0.37 ms^{-1} for the 03 and 04 September events and between 0.44 and 0.48 ms^{-1} for the 31 August and 01 September events, compared to 0.25 ms^{-1} for the Jordan event (Figures 3b and 3c and Table 1). Despite the lower solar radiation in Iceland, the net radiation obtained from the four-component net radiometer was greater than in Jordan due to the lower surface albedo (darker surface), which limited the thermal surface radiation (see Figure 3d). The daytime sensible heat flux was slightly greater in Jordan and the latent heat flux was nearly zero. Conversely, the Icelandic site exhibited a slightly larger latent heat flux than sensible heat flux, which reflects the higher ground surface humidity driven by the daily glacier water discharge. The midday amplitude of the latent heat flux remained similar between events relative to the solar radiation. Additionally, the air in Iceland had a

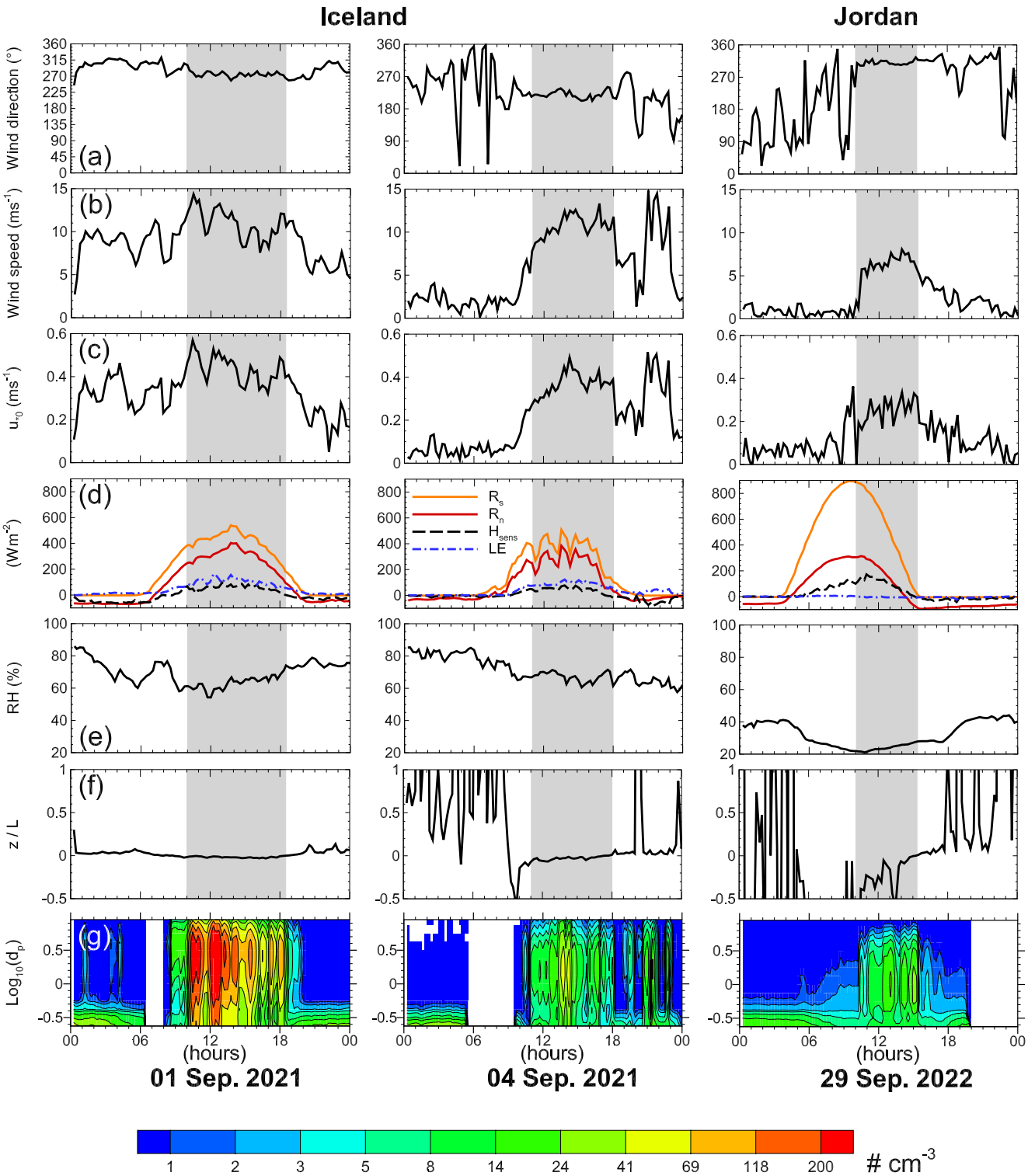

Figure 3. Main characteristics of the 01 and 04 September erosion events in Iceland and 29 September event in Jordan at 2.7–3.0 m height, respectively: time variations of the (a) mean wind direction, (b) mean wind speed, (c) surface friction velocity (u_{*0}) deduced from the sonic anemometers according to Dupont et al. (2018), (d) energy balance including the solar radiation R_s, the net radiation R_n, the sensible heat flux H_{sens}, and the latent heat flux LE, (e) relative humidity RH, (f) thermal stability parameter z/L, and (g) mean size-resolved dust concentration in number. The shaded areas highlight the erosion periods. Characteristics of the 31 August and 03 September events in Iceland are presented in Figure S1 of Supporting Information S1.

Table 1
Main Characteristics of the Selected Erosion Events: Surface Friction Velocity (u_{*0}), 3-m High Wind Speed (U), 3-m High Wind Direction (Wind Dir.), 3-m High Thermal Stability (z/L), and 0.5-m High Relative Humidity (RH)

Campaigns	Events (time in UTC)	u_{*0} (ms^{-1})	U (ms^{-1})	Wind dir. (°)	z/L	RH (%)
Iceland	31 August 09:30–17:00	0.48 (±0.03)	13.0 (±0.7)	270 (±4)	−0.01 (±0.01)	73 (±1)
Iceland	01 September 10:00–18:30	0.44 (±0.07)	10.9 (±1.8)	275 (±6)	−0.02 (±0.01)	63 (±4)
Iceland	03 September 12:30–16:30	0.32 (±0.04)	8.1 (±1.0)	272 (±9)	−0.02 (±0.01)	67 (±5)
Iceland	04 September 11:00–17:30	0.37 (±0.05)	10.8 (±1.2)	220 (±11)	−0.03 (±0.02)	67 (±3)
Jordan	29 September 10:00–15:30	0.25 (±0.05)	6.2 (±1.4)	310 (±6)	−0.35 (±0.73)	24 (±2)

Note. Between parentheses are indicated the standard deviations. Note that results from the 31 August, and 03 September events in Iceland are presented hereafter in Supporting Information S1, as they are similar to those obtained from the 01 September event.

notably higher relative humidity (RH) of approximately 63%–73%, compared to about 24% in Jordan (Figure 3e and Table 1). During erosion events in Iceland, the thermal stratification remained neutral as a result of the strong wind and small sensible heat flux, meaning that the turbulence of the flow was dominated by a mechanical production induced by the wind shear at the surface (Figure 3f and Table 1). In contrast, the thermal stratification was more unstable in Jordan, where the wind intensity was lower, resulting in a larger buoyancy contribution to turbulence production than in Iceland. The higher wind intensity in Iceland also led to significantly greater dust concentration, especially for the 31 August and 01 September events (Figure 3g and Figure S3g in Supporting Information S1).

2.5. Dust Flux Estimation

The size-resolved dust fluxes F_{wd} were estimated at the three OPC heights over 15-min periods using the EC approach. As in Dupont et al. (2021), two corrections were applied: (a) a time-lag correction on the dust fluctuations for each averaging time (15 min) by maximizing the covariance between the dust concentration and vertical wind velocity fluctuations, and (b) a correction accounting for the missing high-frequency part of the dust flux due to the 1 Hz limit of the dust sensor.

To quantify the missing dust flux at high frequencies, two approaches are considered. A first approach consists at comparing the dust-flux cospectra with the standard cospectrum shape while accounting for an attenuation on the high frequency side due to the slow-response of the OPC (Figure 4a). The high frequency losses of the dust flux were estimated for each event and each particle size bin by calculating the difference Δ_{wd}^{1st} between the averaged dust-flux cospectra and its fitted attenuated parabolic shape (Figure 4a). Here, the superscript 1st refers to the first approach. This correction represents on average about +14% of the EC dust flux for both Iceland and Jordan events and shows no evident pattern with particle size (Figures 4b–4d and Figure S4 in Supporting Information S1) as observed in Dupont et al. (2021). It is worth noting that this correction diminishes with height because the size of the motions driving the dust flux increases with height, and thus their time scale as well.

A second approach consists at estimating the high frequency losses of the dust-flux cospectra using the momentum-flux cospectra. The correction corresponds to the high-frequency difference Δ_{wd}^{2nd} between the averaged dust- and momentum-flux cospectra (Figure 4a). Here, the superscript 2nd refers to the second approach. This second approach assumes that dust and momentum are transported similarly at high frequencies. This is similar to assuming similarity between the dust and momentum turbulent diffusivities as usually considered with the FG approach (Dupont et al., 2021). This approach results in a higher correction than the first approach. On average, Δ_{wd}^{2nd} is larger near the surface, especially in Iceland due to the larger wind. This correction can represent up to +100% of the EC dust flux for both the Iceland and Jordan events and shows no clear trend with particle size as Δ_{wd}^{1st} (Figures 4b–4d and Figure S4 in Supporting Information S1). This higher correction compared to Δ_{wd}^{1st} can be attributed to the momentum-flux cospectra displaying a flatter peak and a shift toward higher frequencies compared to the dust-flux cospectra. It is possible that the high-frequency decrease in the dust-flux cospectra, which is where the standard cospectrum shape is fitted in the initial method, begins prematurely due to attenuation related to the OPC's 1-Hz cut-off frequency.

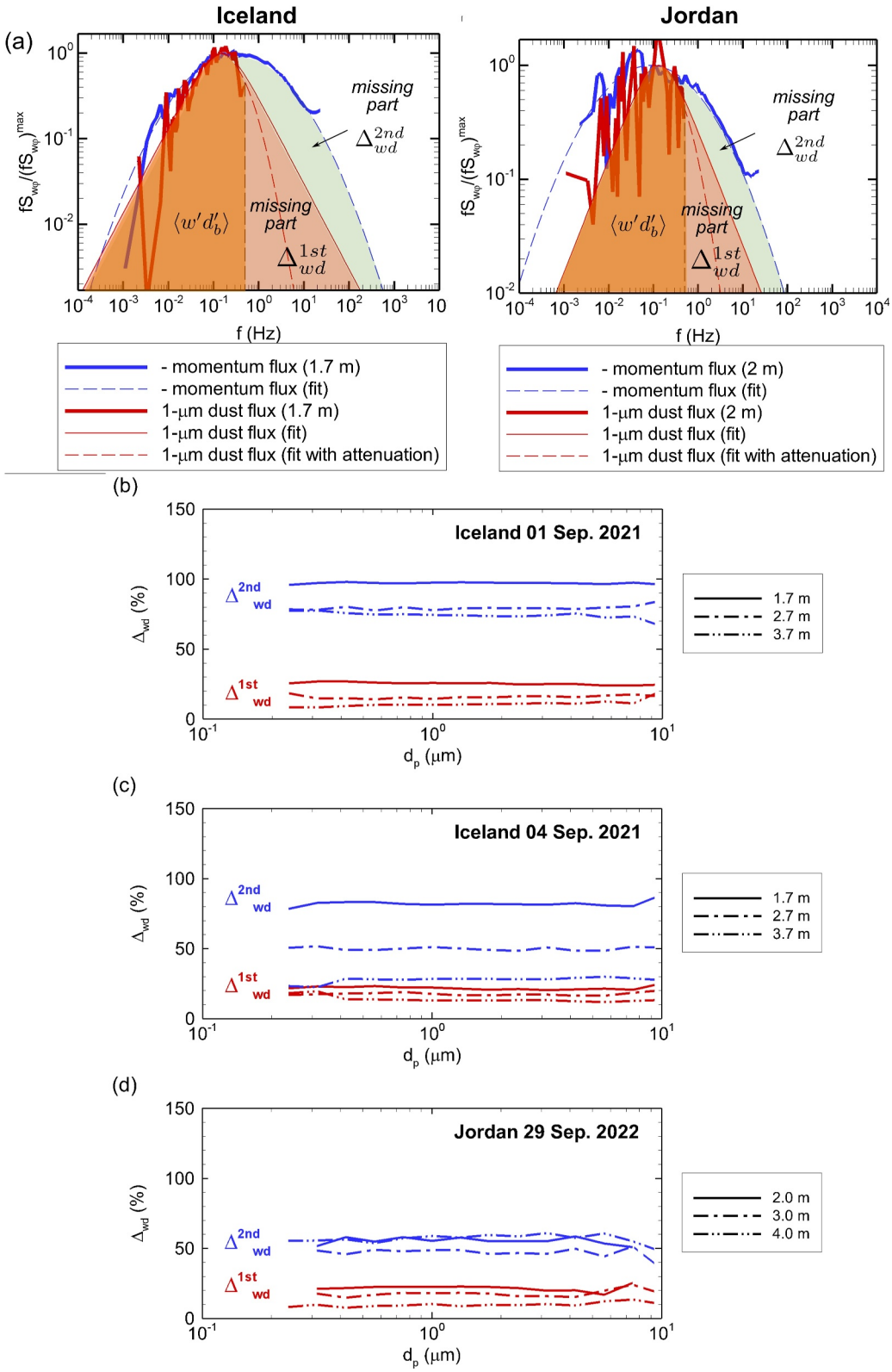

Figure 4.

Without higher-frequency OPCs, it is difficult to determine the correct high-frequency correction between Δ_{wd}^{1st} and Δ_{wd}^{2nd}. Nonetheless, for the purposes of this study, selecting between Δ_{wd}^{1st} and Δ_{wd}^{2nd} corrections should have minimal impact on the comparison of dust fluxes, provided that the same correction method is employed for all dust fluxes. For this study, we applied the Δ_{wd}^{1st} correction.

3. Results

Before investigating the presence of a constant dust flux layer, it is essential to confirm the existence of a near-constant momentum and heat flux layer. The absence of such a layer would suggest that the wind flow releasing and transporting dust is not horizontally homogeneous, with most likely horizontal advection, making a constant dust flux layer improbable. Figure 5 presents for each reference erosion event the time variation of the local friction velocity u_* (square-root of the absolute momentum flux) and sensible heat flux H_{sens}, both at the location of the sonic anemometers, from 0.7 to 3.7 AGL in Iceland and from 2.0 to 4.0 m AGL in Jordan. Note that although the sonic anemometers sampled at a frequency of 50 Hz, a correction for high-frequency losses has been applied to both u_* and H_{sens} in Iceland, in the same way as for the dust fluxes to account for the missing momentum and heat carried by eddies with smaller time scales than the anemometer sampling rate (first approach in Section 2.5). These high-frequency losses in Iceland occur due to the strong wind speeds during the erosion events. They represent at most 10%–30% of the flux for the 0.7-m high momentum and heat fluxes, respectively, and they decrease with height to become negligible above 2.7 m height (Figure S5 in Supporting Information S1). In Jordan, the high-frequency losses of the momentum and heat fluxes were negligible because of the lower wind speed, the smaller eddies carrying momentum and heat having a larger time scale (Table 1 and Figure 2). Overall, both u_* and H_{sens} exhibit a small variability with height, less than 10% of their amplitude. As height increases, u_* tends to slightly increase, while H_{sens} shows a less discernible trend. The same results are observed for the 31 August and 03 September events in Iceland (see Figure S6 in Supporting Information S1). These observations suggest a constant momentum and heat flux layer during all erosion events and thus a horizontally homogeneous flow near the surface.

Regarding the constant dust flux layer, Figure 6 presents for the same erosion events the time variation of the dust flux in number at three heights, from 1.7 to 3.7 AGL in Iceland and from 2.0 to 4.0 m AGL in Jordan. The dust flux is partitioned in four particle size ranges: super-fine dust particles (0.2–0.3 μm), fine particles (0.4–1.0 μm), medium-size particles (1.3–3.2 μm), and coarse particles (4.2–9.0 μm). Due to the stronger wind speed during the 01 September event in Iceland, the dust flux is almost 10 times larger for all particle size ranges than during the 04 September event in Iceland and the 29 September event in Jordan. These last two events exhibit lower dust fluxes of similar amplitude, although the 04 September event had larger friction velocities. The same is observed for the 03 September event in Iceland for a similar friction velocity magnitude (Figure S7 in Supporting Information S1). The most notable contrast between events is the consistently greater amplitude of the dust flux close to the surface (1.7 m AGL) during the 01 September event in Iceland. This is observed for all four particle size categories. The above fluxes at 2.7–3.7 m AGL are lower by a factor of 4–5 and about equal to each other, with the 2.7 m high flux slightly larger than the 3.7 m high flux. The same behavior is observed during the two others westerly Icelandic events on 31 August and 03 September (Figure S7 in Supporting Information S1). On the other hand, during the southwesterly event (04 September) and more notably during the Jordanian event, the dust fluxes exhibit comparable amplitudes at all three heights, except for the super-fine particle size range during the Jordan event, where the 2-m high flux is lower. This result shows an absence of a constant dust flux layer in Iceland below 2.7 m AGL during westerly events, a closer constant dust flux layer during the southwesterly event, and a relatively well-defined constant dust flux layer during the Jordan event, except for the super-fine particle size range for this later event.

Figure 4. (a) Illustration for the 01 September event in Iceland and 29 September event in Jordan of the high-frequency correction of the 1.0 μm-dust flux at 1.7–2.0 m high, respectively, estimated from its cospectrum (S_{wd}) and compared to the momentum flux cospectrum (S_{uw}) at the same heights. The missing part Δ_{wd}^{1st} refers to the high-frequency correction deduced from a standard cospectrum shape fitted on the obtained dust flux cospectrum (thin solid red line), while the missing part Δ_{wd}^{2nd} refers to the high-frequency correction deduced by comparing the dust flux cospectrum with the momentum flux cospectrum. (b)–(d) Variation of the high-frequency corrections of the dust flux as a function of the particle size, when corrections are either based on an extrapolation of the dust-flux cospectra $\left(\Delta_{wd}^{1st}\right)$ or on the momentum flux cospectra $\left(\Delta_{wd}^{2nd}\right)$, for the two Iceland erosion events and the Jordan erosion event, and for the three levels of OPCs. See Section 2.5 for further details. High-frequency corrections of the dust fluxes for the 31 August and 03 September events in Iceland are presented in Figure S4 of Supporting Information S1.

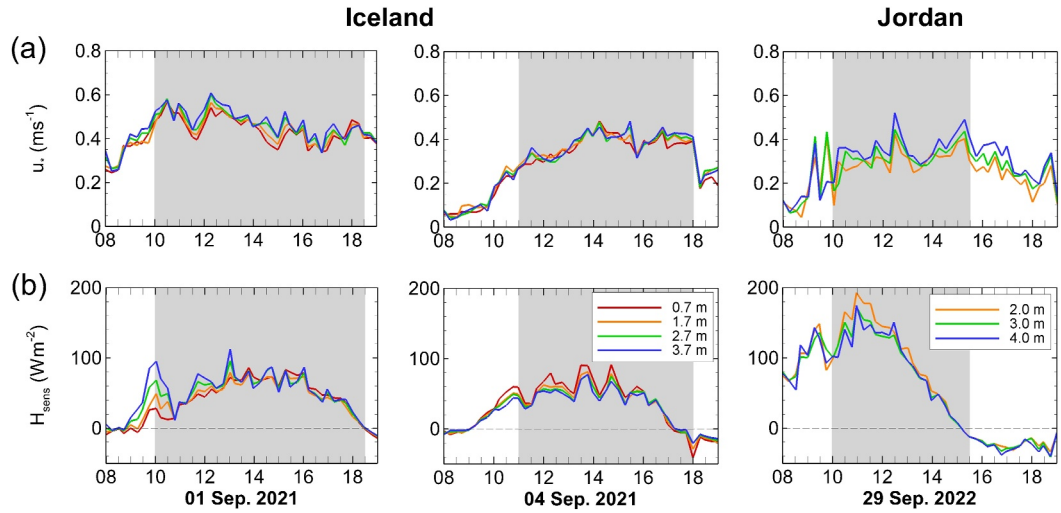

Figure 5. Time variation of the local friction velocity u_* (a) and sensible heat flux H_{sens} (b) at different heights above the surface for the 01 and 04 September events in Iceland and 29 September event in Jordan. The shaded areas highlight the erosion periods. Both u_* and H_{sens} were obtained by eddy covariance from the sonic anemometers. The same figure is presented for the 31 August and 03 September in Iceland in Figure S6 of Supporting Information S1.

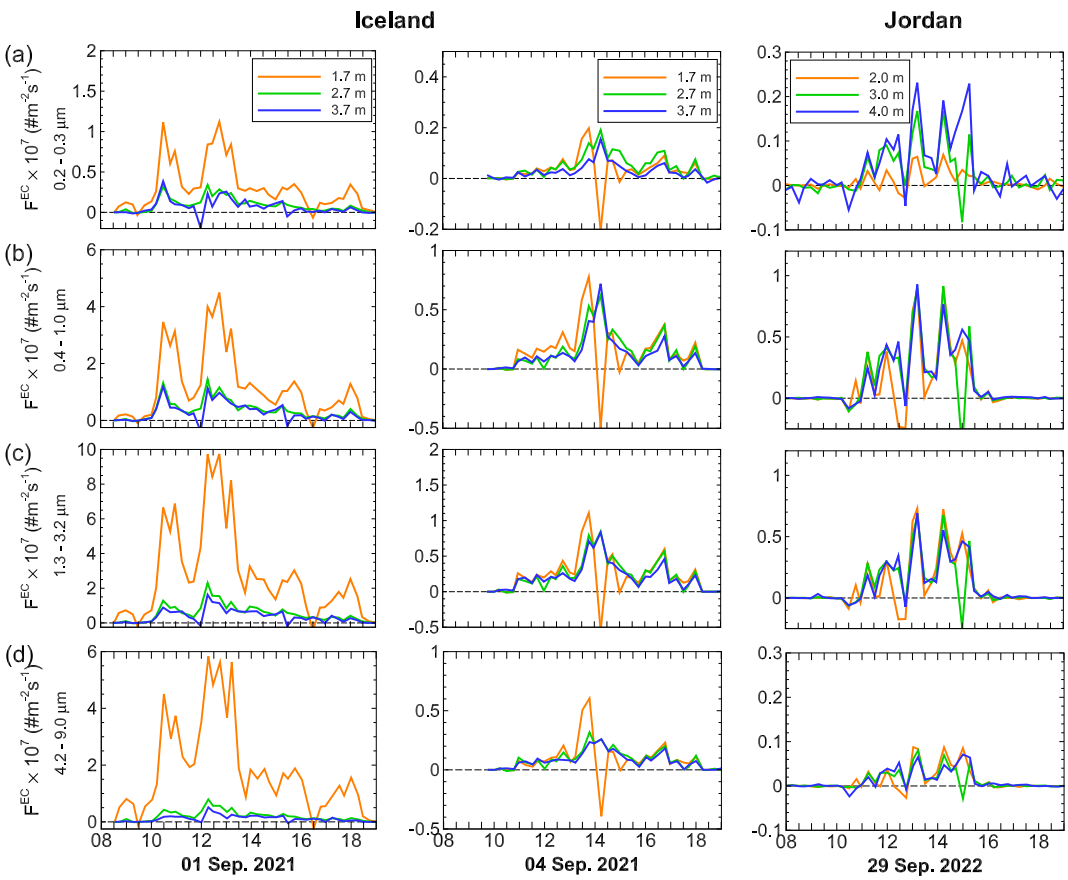

Figure 6. Comparison of the dust fluxes between heights as a function of time during the 01 and 04 September events in Iceland and 29 September event in Jordan. Dust fluxes are in number and for four particle size ranges: 0.2–0.3 µm (a), 0.4–1.0 µm (b), 1.3–3.2 µm (c), and 4.2–9.0 µm (d). The same figure is presented for the 31 August and 03 September in Iceland in Figure S7 of Supporting Information S1.

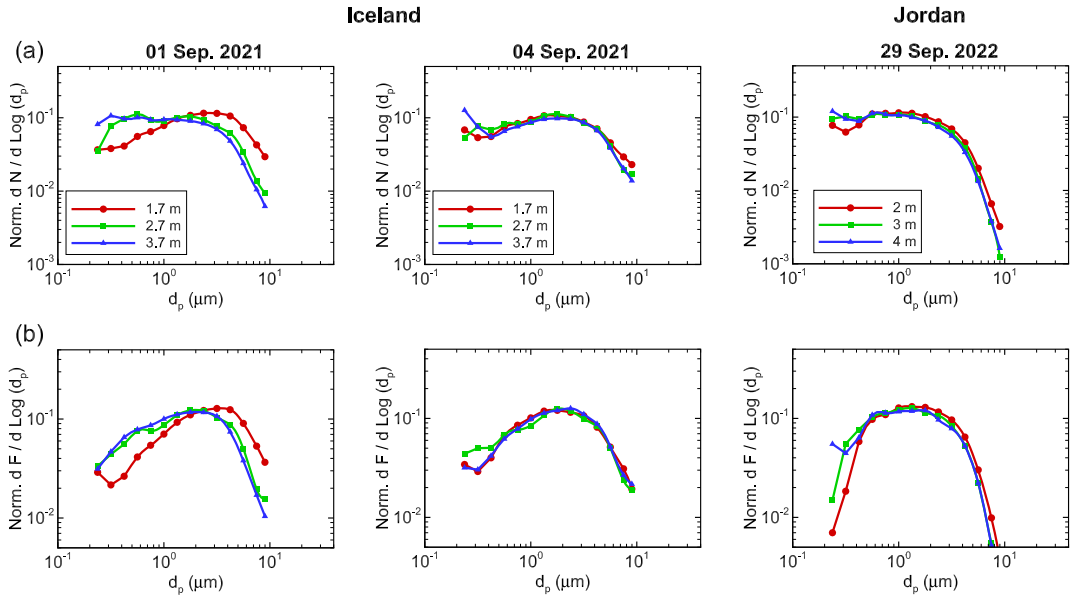

Figure 7. Comparison of ensemble-averaged size distributions of the dust concentration (a) and fluxes (b) in number between different height above the surface, for the 01 and 04 September events in Iceland and 29 September event in Jordan. Ensemble-averages were performed over all 15-min periods during the erosion event. The same figure is presented for the 31 August and 03 September in Iceland in Figure S8 of Supporting Information S1.

Figure 7 presents the normalized ensemble-averaged particle size distributions (PSD) of dust concentrations and fluxes in number, at the three heights, and for the reference erosion events. During the 01 September event in Iceland, the dust concentration PSDs exhibit a mode around 4 µm (Figure 7a). The contribution of this mode decreases with height, as the proportion of submicron particles increases. The same is observed for the two other westerly events in Iceland (Figure S8a in Supporting Information S1). Similarly, for these three westerly events, the dust flux PSDs near the surface (1.7 m AGL) vary in shape from those above at 2.7–3.7 m AGL (Figure 7b and Figure S8b in Supporting Information S1). The dust flux PSDs at 1.7 m AGL are comparable between these three events in Iceland, showing a single mode distribution centered around 4 µm. Further above the ground, the main mode is shifted around 2 µm and a second mode appears around 0.4 µm. The proportion of these two modes varies across the events, with equal contributions during the 31 August event and a greater contribution of the coarser mode during the 01–03 September events. In contrast, the dust concentration and dust flux PSDs of the 04–29 September events in Iceland and Jordan, respectively, show similar shapes with increasing height, with a main mode around 2 and 1 µm for the dust flux, respectively.

4. Discussion and Conclusion

During Icelandic westerly events, the dust fluxes close to the surface were found larger and their PSDs coarser than the ones further above. A southwesterly event showed a more constant dust flux layer. These results challenge the common hypothesis of a constant dust flux layer in the atmospheric surface layer. In contrast, measurements taken during a Jordanian event over similar heights showed near-constant dust fluxes. The absence of a constant dust flux layer in some of the events in Iceland is further analyzed in this section.

4.1. Some Possible Causes to Exclude

Several possible causes for observing higher dust fluxes near the surface in Iceland can be excluded. First, the corrections applied to the dust fluxes unlikely explain the difference in fluxes with height. The difference of dust flux corrections with height represented only a small percentage of the flux (less than 20% according to Figure 4b) while the fluxes varied up to 400% with height. Second, a particle settling flux adding to the diffusive dust flux with increasing particles size could not be the reason for weakening the constant dust flux layer because (a) the gravitational settling flux estimated as the particle settling velocity times the particle concentration, represented less than 5% of the diffusive flux, and (b) the difference of dust fluxes with height was observed for all particle

sizes, including particle sizes with negligible settling velocities (submicron particles). Third, a difference in flow characteristics with height due to a limited extent of the site surface homogeneity (i.e., limited fetch) is also improbable as the momentum and heat fluxes were observed to be constant with height for westerly and southwesterly wind sectors. This last observation means that the upwind surface of the measurement mast was homogeneous in term of momentum absorption and heat release. An estimate of the flux footprints at the three measurement heights (estimated according to Kljun et al. (2015)) indicates that over 60% of the fluxes at these heights originate from an apparently homogeneous surface during all erosion events (See Figure 1a for the footprints of the 01–04 September events in Iceland). According to this footprint analysis, an upwind lava field with stronger roughness and probably lower dust emission than the surrounding surface of the mast might have affected the upper fluxes (3.7 m high) during westerly wind events. Nevertheless, as this upwind lava field had little impact on the upper momentum and heat fluxes, it is unlikely to have significant effects on the upper dust fluxes during westerly winds. This cannot explain the 400% difference between the lower and upper dust fluxes. Additionally, it would not elucidate the significant variation in dust fluxes between the two lower levels at 1.7 and 2.7 m height.

4.2. Hypothesis of a Dust Roughness Sublayer (DRSL)

We hypothesize that the absence of a constant dust flux layer in Iceland is explained by the existence of a dust roughness sublayer (DRSL), referred to hereafter as DRSL, due to the spatial heterogeneity or patchiness of the dust source. As shown in Figure 1a, the flux footprints change (a) with wind direction as the source area contributing to the flux covers a different region of the surface, and (b) with height as the source area becomes larger and extends further upwind with increasing height. In presence of surface dust source inhomogeneities, dust concentrations profiles can exhibit irregularities with height, differing from the expected decreasing profiles with height, as the consequence of interactions between plumes emanating from different surface dust sources (H. Butler et al., 1996; H. J. Butler et al., 2005). Similarly, the magnitude of the dust flux can vary with height and wind direction according to the covered source area. In Iceland, the ground surface was more humid than in Jordan as shown by the larger water vapor flux in Iceland (see the latent heat flux in Figure 2d). Furthermore, erosion events in Iceland occurred a few days after a site flooding caused by the nearby glacier melting, which has further accentuated the surface humidity. On the site, fixed patches of drier ground surface were observed to emit more dust than the surrounding wetter surfaces. These patches spanned several meters and expanded slowly over time as the surface became drier due to strong winds and the absence of rain and additional flooding. We suspect that this spatial variability in surface humidity resulted in a greater contrast in dust emission than in heat flux between wet and dry surfaces, enhanced by the threshold mechanism of dust emission, explaining the observed constant heat flux layer. These surface conditions differ from those in Jordan where the soil was dry, with very minimal water vapor flux, and the dust emissions were not initiated from fixed locations like in Iceland, but from source patches moving as the gusts swept and scratched the surface.

To explain the systematic larger dust flux near the surface in Iceland during westerly winds, we suspect that the near-surface OPC (1.7 m high) was located in the wake (plume) of a surface dust source patch for this wind direction, as illustrated in Figure 8, while the upper OPCs were located above a dust blending height above which the local influence of individual surface dust patches decreases as the dust becomes spatially mixed. During southwesterly winds, the near-surface OPC was located in-between or far from the wakes (plumes) of intense surface dust source patches, which would explain the closer constant dust flux layer to the surface for this wind direction. In Iceland, the near-surface OPC was therefore located within a DRSL, by analogy with the momentum roughness sublayer in heterogeneous surfaces (Raupach et al., 1991), where the time-average dust concentration is not horizontally homogeneous and where the dust flux differs according to the wind direction, due to the patchiness of the dust source. There, the vertical dust flux should not be constant with height because of the non-negligible horizontal dust advection. The location of the two upper OPCs above the dust blending height would explain the similar dust fluxes observed from these two OPCs, independently of the wind direction. At the dust blending height, turbulent diffusion is expected to dominate the vertical dust exchange.

4.3. Support for DRSL Hypothesis Based on the Dust Concentration

To support the hypothesis that the lower OPC in Iceland was located in a DRSL, we examined the correlation in dust concentration between OPCs, and the skewness and kurtosis of dust concentration fluctuations, all evaluated over 15 min periods for each particle size bin. If the lower OPC was situated within a DRSL and the two upper

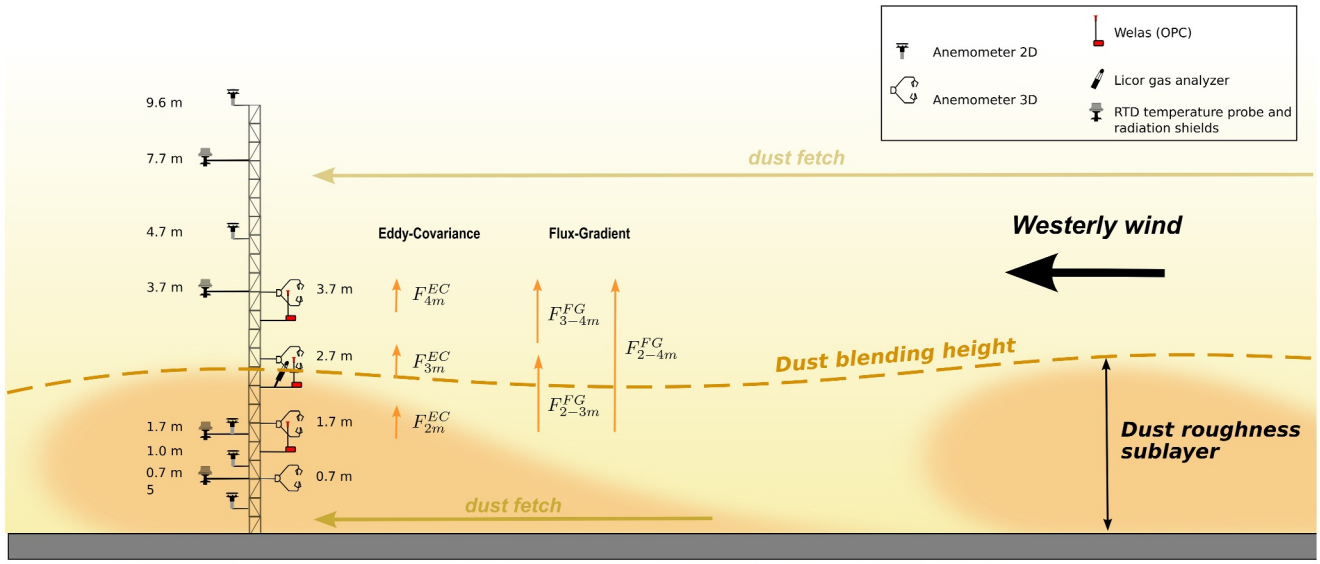

Figure 8. Schematic illustration depicting the suspected presence of fixed surface dust source patches on the Icelandic site resulting from heterogeneous surface humidity. These patches lead to the formation of a thick dust roughness sublayer where the dust concentration is spatially heterogeneous. Once the dust blending height is surpassed, estimated to be between 2 and 3 m above the ground, the dust concentration becomes spatially mixed and the dust flux remains near-constant with increasing height. Dust fluxes are estimated at the three optical particle counters heights using the eddy covariance (EC) methods. These EC dust fluxes are compared with dust fluxes estimated from the flux-gradient (FG) method using three combinations of two OPCs as represented in this scheme (see Figures 12 and 13).

OPCs were located above a dust blending height, then the correlation in concentration between the lower and the two upper OPCs should be less than that between the two upper OPCs. Additionally, the DRSL dust concentration should be more intermittent compared to above the dust blending height. This is because dust is less spatially dispersed within the DRSL, and its concentration is more sensitive to wind direction. The dust concentration skewness and kurtosis of the two upper OPCs should be smaller and closer to Gaussian values than those obtained from the lower OPC.

Figure 9 presents the temporal variation of the size-resolved concentration correlations between the lowest and middle height OPCs, as well as between the middle and highest height OPCs, for reference Icelandic and Jordanian events. Other westerly Icelandic events are shown in Figure S9 in Supporting Information S1. The figures provide evidence that for the westerly Icelandic events, the correlation between the lowest and middle height OPCs is lower than the correlation between the two upper OPCs. Conversely, in Jordan, the correlations between the three OPCs are similar. The Icelandic southwesterly event exhibits intermediate behavior, with a slightly lower correlation between the two lower OPCs. This implies that the near-surface OPC in Iceland was not within the same dust layer as the two upper OPCs, or at least not during westerly winds.

Figure 10 shows the skewness and kurtosis of the size-resolved dust concentrations at the three OPC heights and for reference Icelandic and Jordanian events (see Figure S10 in Supporting Information S1 for other westerly Icelandic events). As expected, the low wind events exhibit higher skewness and kurtosis at all heights as the event intensity is close to the erosion threshold, resulting in more intermittency. For the same reasons, the beginning and end of intense events show larger skewness and kurtosis at all heights as the wind is lower and the erosion more intermittent. Interestingly, the dust concentrations during the Icelandic westerly events show a decrease in skewness and kurtosis with increasing height. Notably, the blue color delimited by a dashed white isoline (representing low values) intensifies and expands toward coarser particles during these events. This stands in contrast to the relatively consistent color with height observed during the southwesterly Icelandic and Jordanian events. This confirms that the dust concentration fluctuations were less intermittent and approached a Gaussian distribution with increasing height during westerly events in Iceland, supporting the idea that the dust concentration was more spatially mixed with increasing height for this wind sector while the dust concentration was decreasing.

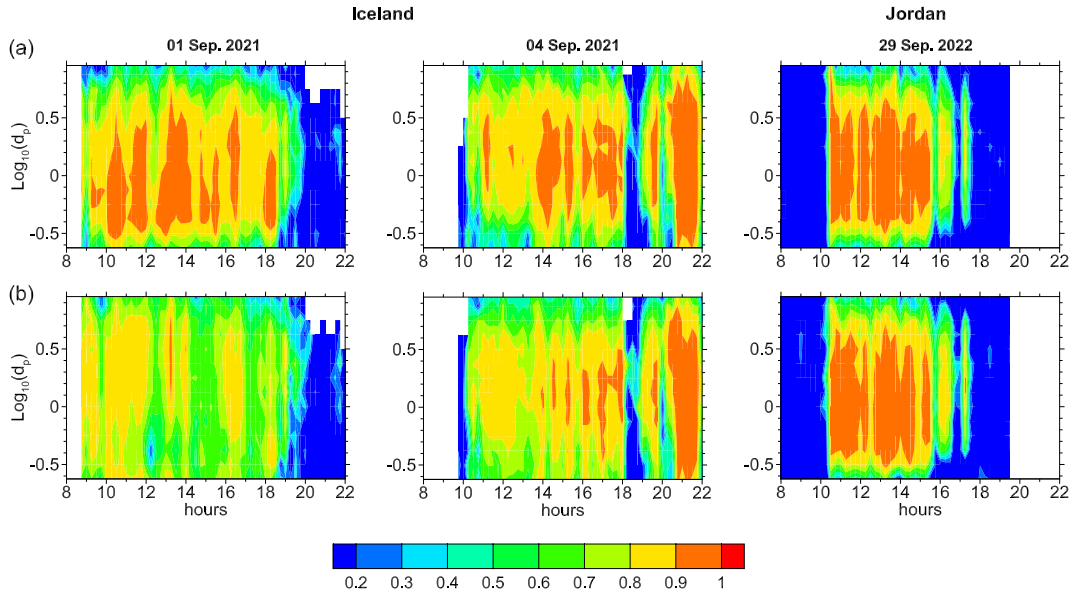

Figure 9. Time variation of the size-resolved dust concentration correlation coefficients estimated over 15 min periods, between the middle and highest height OPCs (top figures) and between the lowest and middle height OPCs (bottom figures), for the 01 and 04 September events in Iceland and 29 September event in Jordan. A perfect correlation would give a coefficient equal to one. The blank values correspond to periods when the OPCs were not working or to size bins where no particles were detected. The same figure is presented for the 31 August and 03 September in Iceland in Figure S9 of Supporting Information S1.

4.4. Support for DRSL Hypothesis Based on the Dust Flux

To support the hypothesis of a DRSL, we also evaluated the sensitivity of the relationship between the dust flux F^{EC} and the surface friction velocity u_{*0}, to the height and wind direction. Above the DRSL, this relationship should become independent of the wind direction since the dust flux ought to integrate the patchiness of the surface dust sources. This assumes that the threshold friction velocity u_{*h} above which dust emission started, is also independent of the wind direction.

Figure 11 displays F^{EC} as a function of u_{*0} for four particle size ranges, three OPC heights and for the four Icelandic events and the Jordanian event. In agreement with earlier research (e.g., Ishizuka et al., 2014), F^{EC} appears proportional to u_{*0}^{n}, where n was chosen here equal to 4 as in Gillette and Passi (1988). The Jordanian event shows little variation with height of the relation between F^{EC} and u_{*0}. The fitted curves are close to each other. This is consistent with the presence of a constant dust flux layer. The Jordanian event exhibits also a lower u_{*h} than Icelandic events due to a lower soil surface humidity. Here, u_{*h} is estimated as the u_{*0} value at which the fitted curves F^{EC} versus u_{*0} intersect with negligible dust flux values, which were approximated here as $F^{EC} = 10^4$ and 10^5 # $m^{-2}s^{-1}$ in Jordan and Iceland, respectively. This lower u_{*h} in Jordan explains the larger levels of dust flux values in Jordan for equivalent u_{*0}. For Icelandic events, the relation between F^{EC} and u_{*0} shows more variation. The first Icelandic event (31 August) exhibits a greater u_{*h} than subsequent events. This greater value of u_{*h} is observed across all heights and particle sizes, with u_{*h} around 0.40 ms^{-1} against 0.20–0.25 ms^{-1} for the subsequent Icelandic events. This decrease of u_{*h} is thought to be related to surface drying, which appears more pronounced between 31 August and 01 September. In fact, at the beginning of the 01 September event, F^{EC} displayed the same relation with u_{*0} as during the 31 August event, but as the surface became drier during the event, the value of F^{EC} increased for equal u_{*0} (result not shown).

For Icelandic events with close u_{*h} values (01–04 September events), the relationship between F^{EC} and u_{*0} is relatively consistent between events for the two upper OPCs, regardless of wind direction, the fitted curves and dots being close to each other as during the Jordanian event. This suggests that these heights were above the dust blending height as the dust fluxes were spatially homogeneous, regardless of wind direction. The patchiness of surface dust source disappeared at these two heights. On the other hand, for the lower OPC, the relationship obtained for the southwesterly event diverges from that obtained for the westerly events. Notably, the fitted curves

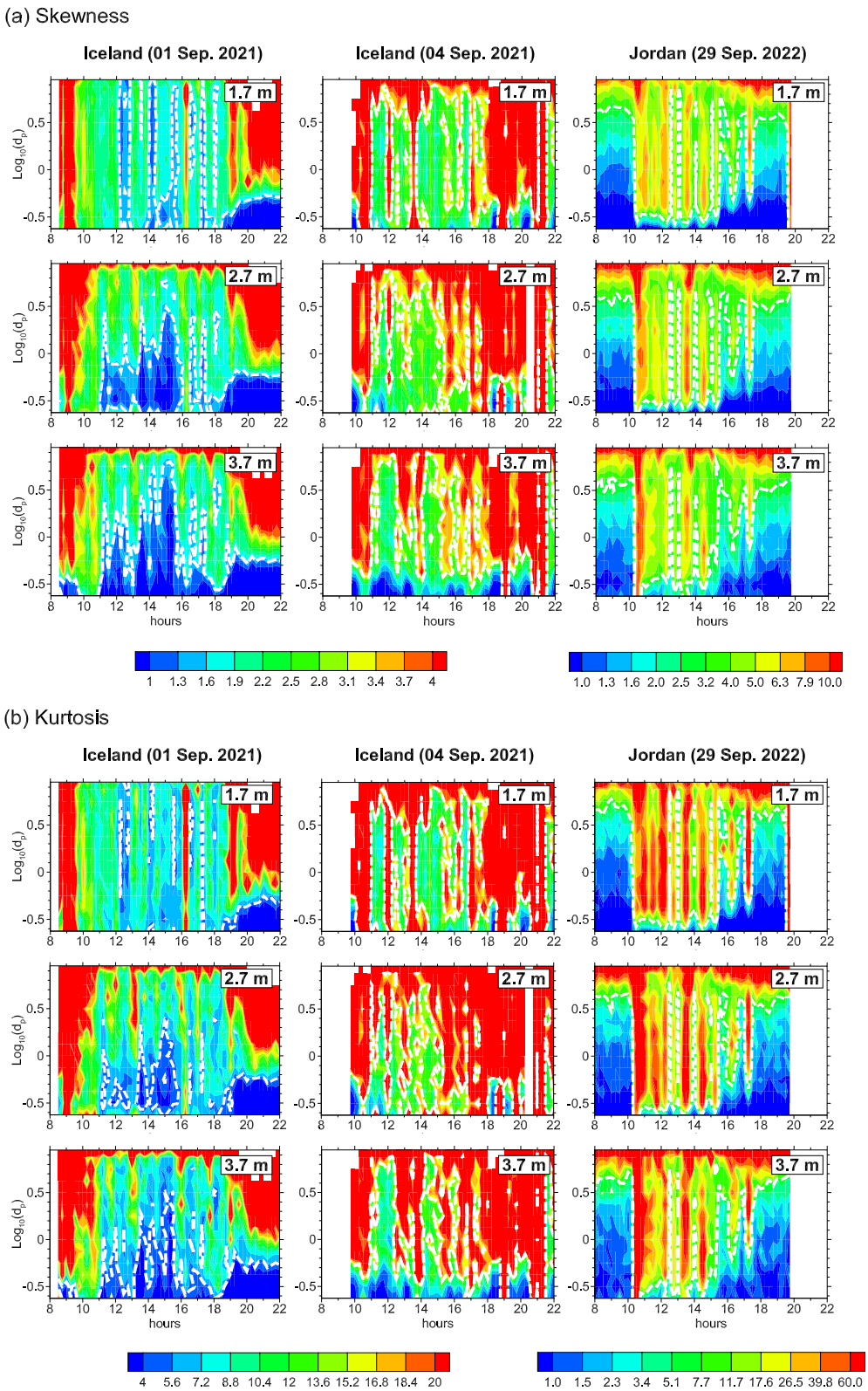

Figure 10.

seem less clustered together than those at the upper two heights. For equivalent u_{*0}, the southwesterly event exhibits lower dust fluxes than the westerly events, 01 and 03 September events. This last result supports the idea that the near-surface OPC was located downstream a dust source patch during westerly winds, and more generally was located within the DRSL, where the relationship between F^{EC} and u_{*0} differs with wind direction, depending on the distance to the upwind dust source patches.

4.5. Dust Flux Particle Size Distribution

Within the DRSL, the dust flux PSDs appeared richer in coarse particles when measurements were taken downstream of a dust source patch (i.e., westerly vs. southwesterly events), and richer also than fluxes captured above the DRSL (Figure 7 and Figure S8 in Supporting Information S1). We attribute this difference in PSD by a lower contribution of the diffusive deposition flux of coarse particles relative to their emission flux when measurements were taken in the wake of a dust source. There, the dust fetch of the near-surface measurements is expected to be (a) shorter than the fetch of the measurements taken above the DRSL, because the former fetch is dominated by the nearby source patch (see Figure 8), and (b) shorter than the fetch of measurements taken within the DRSL but far from dust source patches (i.e., southwesterly event). According to Fernandes et al. (2019), a longer dust fetch results in dust fluxes richer in fine particles because of the increased contribution of the deposition flux of coarse particles relative to the total diffusive flux as their concentration rises in the air along the fetch. This explanation is reinforced by the observed negligible impact of u_{*0} on the size distributions of DRSL dust fluxes between westerly events (Figure 12 for $z = 1.7$ m). This, indeed, suggests a negligible deposition flux downstream of a dust source patch as the known increase of coarse particle deposition with u_{*0} is not perceptible there on the dust flux PSD.

Above the DRSL, the dust fluxes became progressively richer in coarse particles over time, particularly between 31 August and 01 September (Figure 12a for $z = 2.7$ and 3.7 m). This is probably due to the decrease of u_{*0} during the sequence of erosion events (see Table 1). Unlike within the DRSL, the proportion of coarse particles in dust fluxes above the DRSL exhibits a negative correlation with u_{*0}, with a reduction in the amount of coarse particles as u_{*0} increases (Figure 12b for $z = 2.7$ and 3.7 m). This result is consistent with recent observations made by González-Flórez et al. (2023) during erosion events in Morocco with long dust fetches. As proposed in that earlier study, this reduction in coarse particles with increasing u_{*0} may be attributed to their greater deposition contribution relative to their emission. The alignment of the 31 August event with the other events in terms of proportion of particle size bins in the dust flux as a function of u_{*0} (Figure 12b), disregarding the higher u_{*h} of the 31 August event, further supports this deposition influence rather than an emission cause on the dust flux PSD. This is because deposition should not depend on u_{*h} unlike emission. Thus, dust flux PSD was primarily influenced by u_{*0} through probably deposition, while the dust flux magnitude was influenced by both u_{*0} and u_{*h}.

4.6. Consequences of the Absence of a Constant Dust Flux Layer

The absence of a constant dust flux layer in Iceland has two important consequences. First, while measuring close to the surface is often preferred to obtain larger dust concentrations and a stronger vertical dust gradient, our results in Iceland show that measuring dust concentration too close to the surface could lead, in certain configurations, to values that are not representative of the whole surface. This happens when the dust source is patchy, as in presence of humidity or in presence of non-erodible roughness elements (sparse vegetation, rocks…). Anticipating the depth of the DRSL for estimating the appropriate measurement heights can be challenging. The spatial variability of surface humidity and the size of the dust source patches are more difficult to evaluate, and fluctuating in time, than the size of the dust source patches between the surface roughness elements. Nonetheless, our findings showed that if a strong correlation exists between dust concentration fluctuations recorded at two levels ($\geq$0.9 for the dominant particle size range, according to Figure 9) and if these fluctuations share comparable skewness and kurtosis values, then both levels are probably situated within a constant dust flux layer. Second, the

Figure 10. Skewness (a) and kurtosis (b) of the dust concentration estimated over 15 min periods, at three heights above the ground as a function of time (horizontal axis) and particle size (vertical axis), for the 01 and 04 September events in Iceland and 29 September event in Jordan. The dashed white isolines help to visualize the expand of low skewness and kurtosis values for the westerly Icelandic event (01 September), while for the southwesterly event (04 September) and the Jordanian event (29 September) the isolines do not show specific trend with height. The blank values correspond to periods when the OPCs were not working or to size bins where no particles were detected. The same figure is presented for the 31 August and 03 September in Iceland in Figure S10 of Supporting Information S1.

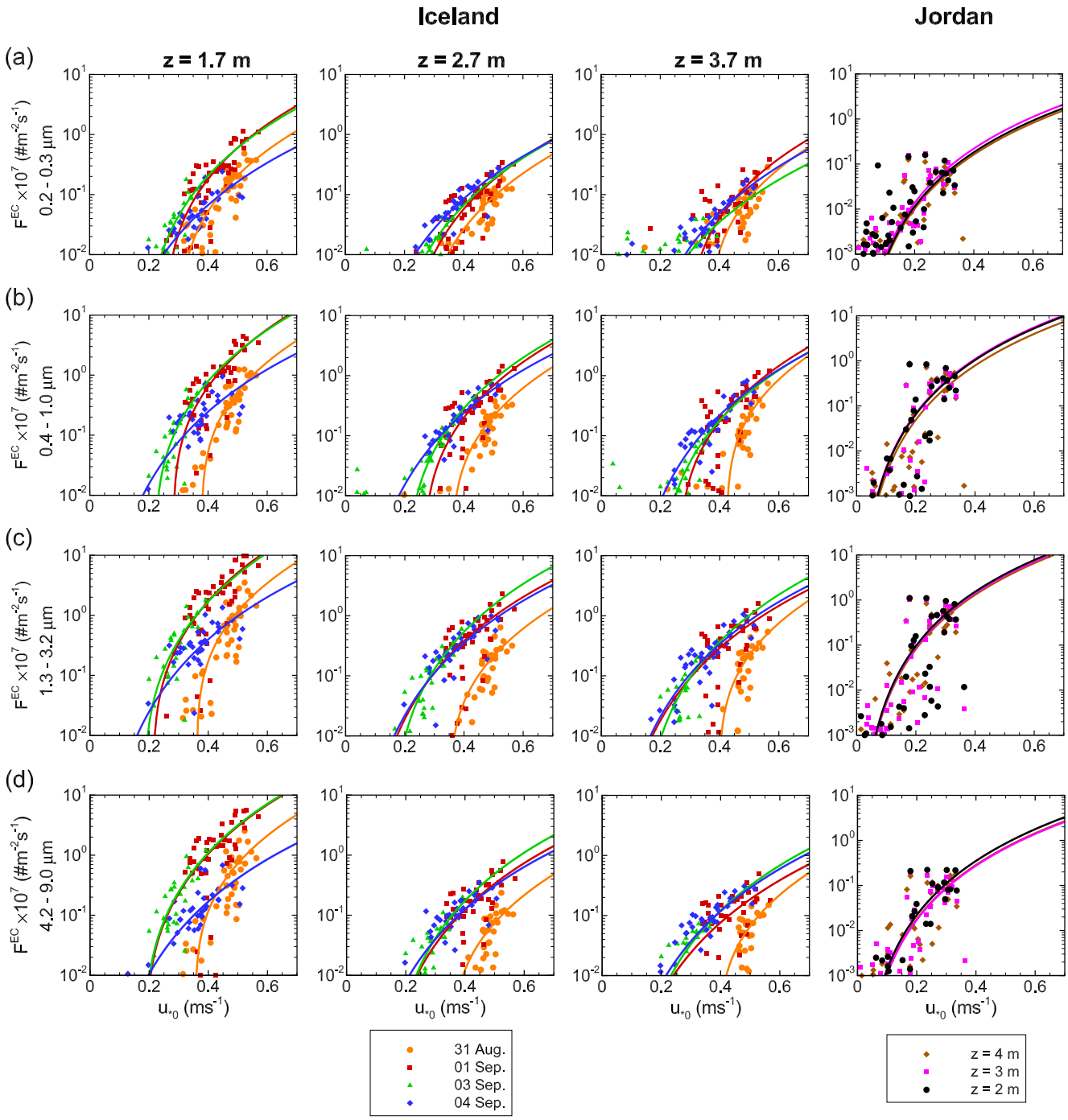

Figure 11. Dust fluxes F^{EC} as a function of the surface friction velocity u_{*0} for all erosion events in Iceland and in Jordan (right figures) and at the three measurement heights. Dust fluxes are in number and for four particle size ranges: 0.2–0.3 µm (a), 0.4–1.0 µm (b), 1.3–3.2 µm (c), and 4.2–9.0 µm (d). The solid curves are fit over each event and each height such as $F^{EC} = \alpha u_{*0}^3 (u_{*0} - \beta)$. The color of these curves corresponds to the color of the associated dots.

estimation of the emission dust flux using the flux-gradient (FG) method between two dust concentration levels representing different dust layers may result in substantial errors in the dust flux value.

To investigate the implications of having a dust measurement level within the DRSL on the estimated FG dust flux, we compared the FG dust fluxes estimated from (a) the two lower OPCs, F^{FG}_{2-3m}, (b) the two extreme OPCs (lower and upper), F^{FG}_{2-4m}, and (c) the two upper OPCs, F^{FG}_{3-4m}, with the EC dust fluxes at the three OPC heights

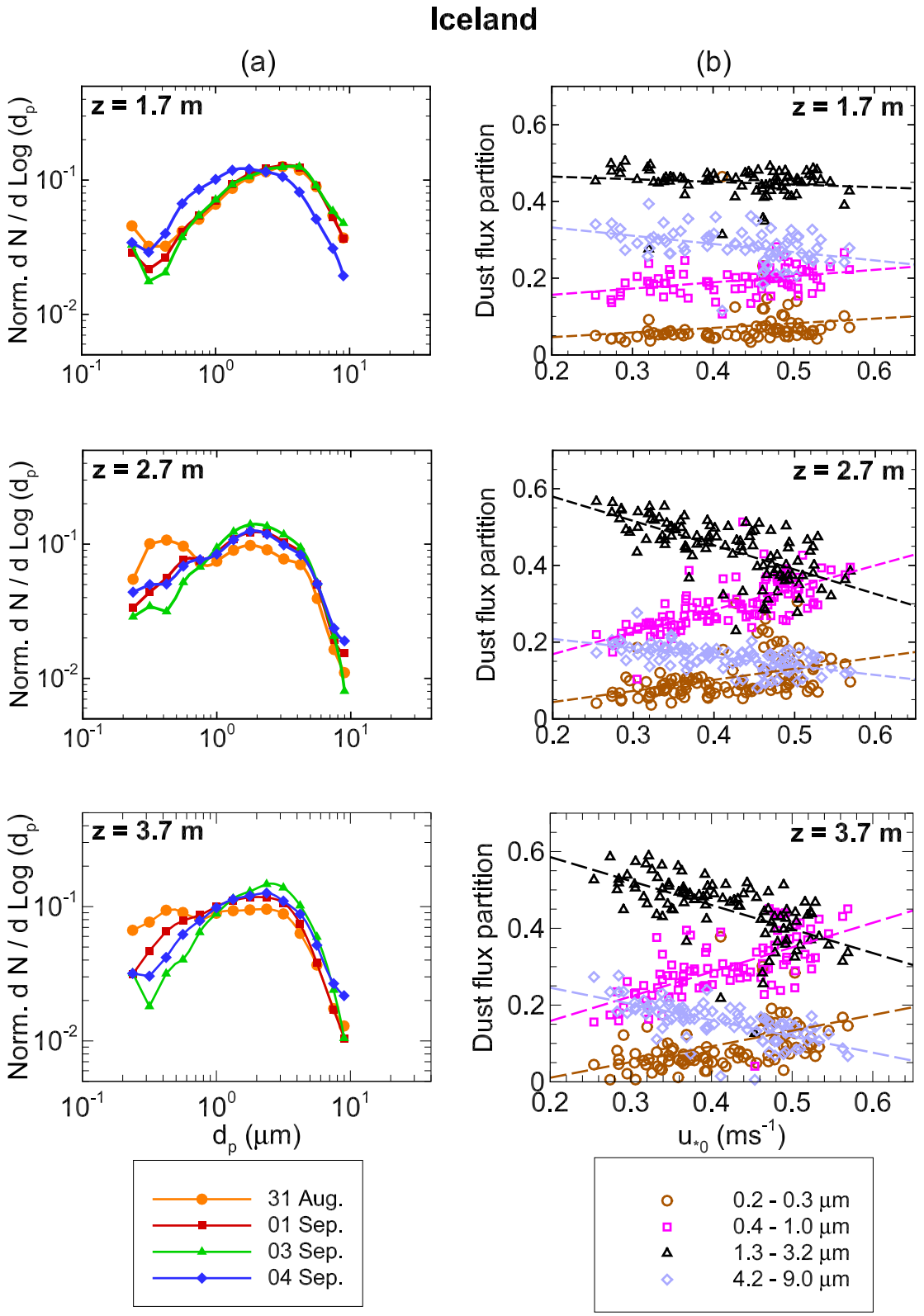

Figure 12. (a) Comparison of ensemble-averaged size distributions of the dust fluxes in number between Icelandic events, for three heights above the surface. Ensemble-averages were performed over all 15-min periods of each erosion event. (b) Partition of the dust flux between size bins as a function of the surface friction velocity u_{*0}, for four particle size bins and three heights above the surface, integrating all Icelandic erosion events, except at z = 1.7 m where the 04 September event was not considered because it was different from the others. Each dot represents one 15-min period. Dashed lines represent linear fit of each particle size range.

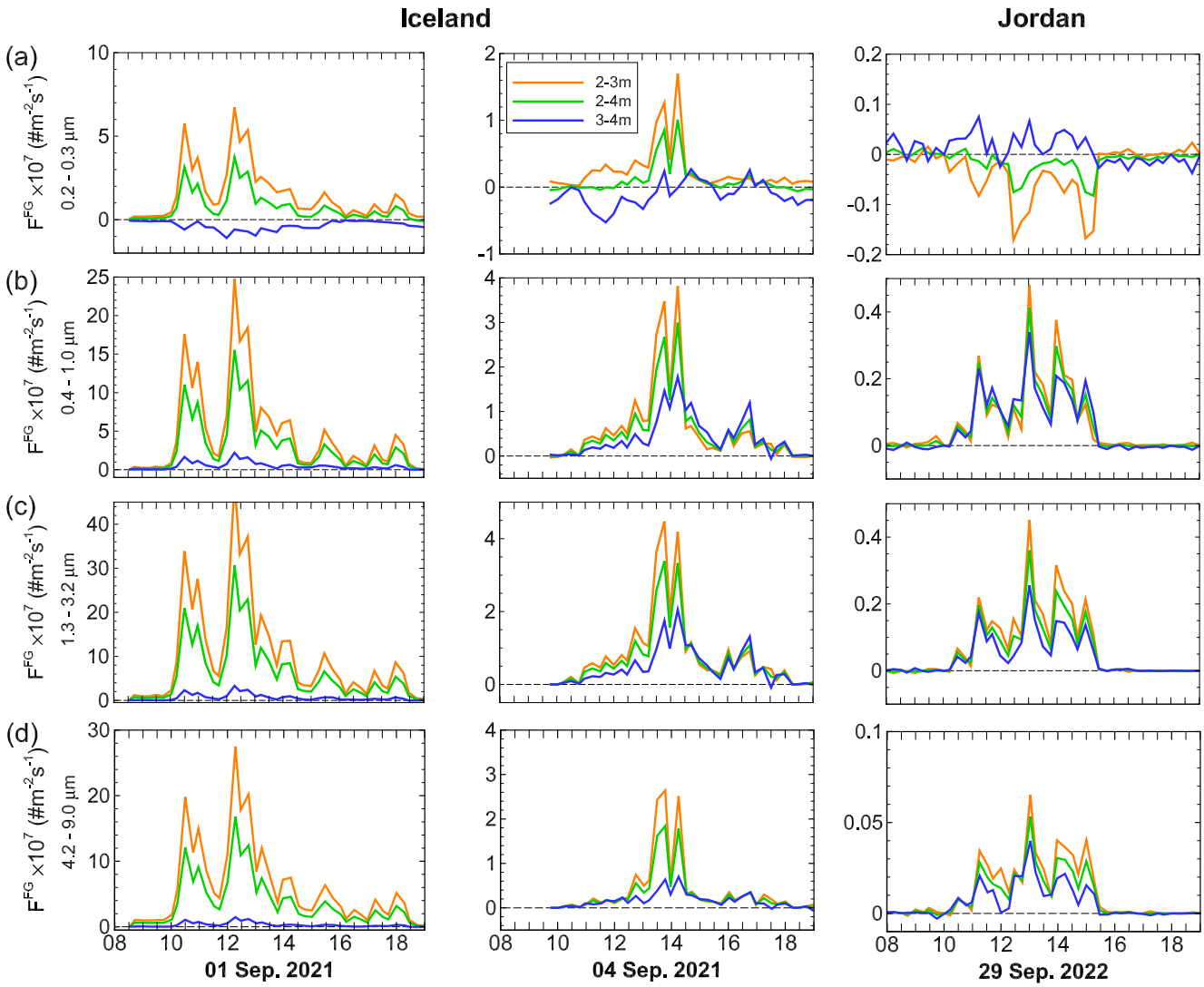

Figure 13. Comparison of the flux-gradient (FG) dust fluxes between heights as a function of time during the 01 and 04 September events in Iceland and 29 September event in Jordan. Dust fluxes are in number and for four particle size ranges: 0.2–0.3 µm (a), 0.4–1.0 µm (b), 1.3–3.2 µm (c), and 4.2–9.0 µm (d). The "2–3 m" FG dust fluxes have been calculated using the two lower OPCs, the "3–4 m" FG dust flux using the two upper OPCs, and the "2–4 m" FG fluxes using the lower and upper OPCs, as illustrated in Figure 8. The same figure is presented for the 31 August and 03 September in Iceland in Figure S11 of Supporting Information S1.

F_{2m}^{EC}, F_{3m}^{EC} and F_{4m}^{EC}, respectively (see Figure 8 for a schematic description). The comparison heights between the FG and EC dust fluxes are not perfectly identical, except between F_{3m}^{EC} and F_{2-4m}^{FG}, but it is sufficient to give an idea on the agreement between the EC and FG dust fluxes. The FG dust fluxes have been corrected for dissimilarity between momentum and dust transports by removing the extra fraction of the normalized momentum flux on the low and high frequency sides compared to the normalized EC dust flux, as done in Dupont et al. (2021). Figure 13 presents the time variation of the FG dust fluxes for the reference Icelandic and Jordanian events. Other westerly Icelandic events are shown in Figure S11 in Supporting Information S1. For fine dust (<0.4 µm), the FG dust fluxes exhibit opposing signs at different heights. This suggests that the difference in dust concentration between OPCs is too small for this particle size range, leading to positive and negative fluxes. For particles larger than 0.4 µm, the FG dust fluxes near the surface are notably higher than the upper fluxes during Icelandic events, while the middle fluxes fall between the two. This difference in fluxes is exacerbated during westerly events. During the Jordanian event, the three FG dust fluxes appear much closer to each other, but the dust flux near the surface remains often higher than the upper flux.

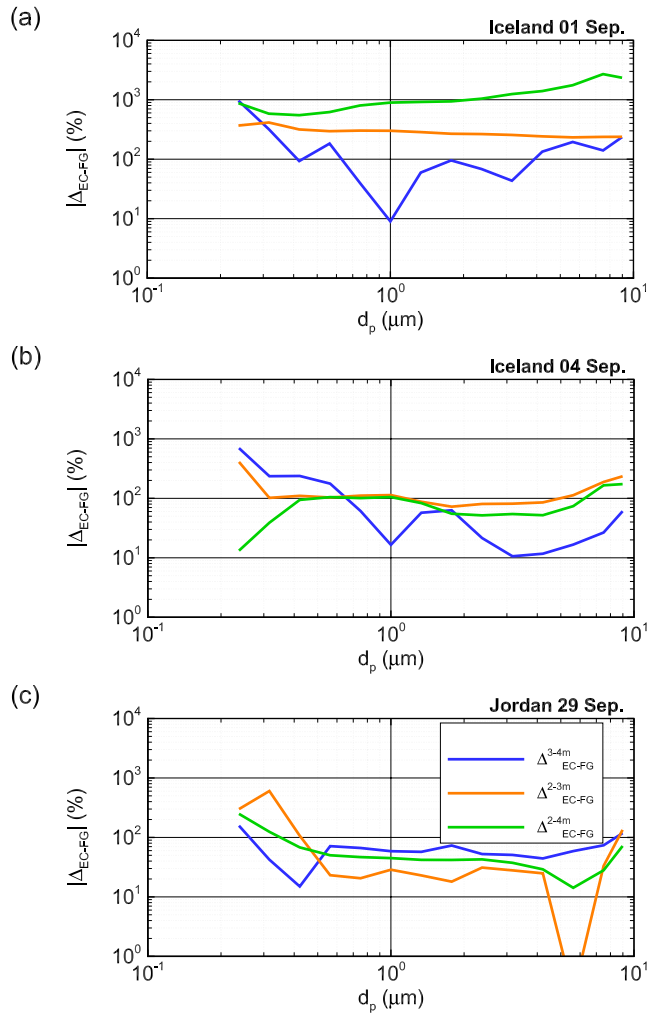

Figure 14. Difference between EC and FG dust fluxes as a function of particle size, for the 01–04 September events in Iceland (a, b) and 29 September event in Jordan (c). The difference is expressed in percentage of the EC dust flux. The "3-4 m" superscript refers to the 3.7–4 m high EC dust fluxes compared to the FG dust fluxes estimated using the 3 and 4 m high OPCs. The "2-3 m" superscript refers to the 1.7–2 m high EC dust fluxes compared to the FG dust fluxes estimated using the 2 and 3 m high OPCs. The "2–4 m" superscript refers to the 2.7–3 m high EC dust fluxes compared to the FG dust fluxes estimated using the 2–4 m high OPCs. See Figure 8 for illustration. The same figure is presented for the 31 August and 03 September in Iceland in Figure S12 of Supporting Information S1.

Figure 14 presents the difference in absolute values between the EC and FG dust fluxes in particle number relative to the EC dust flux, for the three heights and for Icelandic and Jordanian events (see Figure S12 in Supporting Information S1 for other westerly Icelandic events). Compared to the FG dust fluxes, the EC fluxes are overall larger during the Jordanian event and lower during the Icelandic events (Figure 6 compared to Figure 13). During the Jordanian event, the FG and EC dust fluxes exhibit at all heights differences lower than 70% of the EC dust flux for particles between 0.5 and 5.0 µm. These differences are greater than those reported in Dupont et al. (2021) for erosion events in Tunisia, which we cannot explain. For finer and coarser particles, this difference amplifies, possibly due to the lower magnitude of dust concentration. During the Icelandic events, the upper FG dust flux $\left(F^{FG}_{3-4m}\right)$, which does not use the concentration from the lower OPC, remains the closest to the equivalent-height EC dust flux $\left(F^{EC}_{4m}\right)$, for particles between 0.5 and 8.0 µm with difference of the order of 30%–100% of the EC dust flux. The two other FG dust fluxes using the lower OPC appear to be much higher than their corresponding EC fluxes, especially during westerly events, with the difference reaching up to about 1,000%. It is likely that the FG dust fluxes using the dust concentration level located within the DRSL, overestimate the dust flux when this lower level is located downstream of a nearby dust source patch.

4.7. Final Remarks

This study highlighted the contrasting dust emission behavior in two different desert regions, in Iceland and Jordan. The observed differences were primarily due to contrasting surface humidity. The more humid surface conditions in Iceland produced spatial variability of dust emission.

Our results show that, despite an apparent uniformity of an erosive surface, the patchiness of the dust source caused by the soil humidity may enhance the depth of the DRSL. Within the DRSL, dust fluxes are more intermittent and depend on wind direction. They are also non-uniform spatially in magnitude and in size distribution relative to the value of u_{*0}, and the deposition contribution of coarse particles to the dust flux may vary according to the distance of the nearby dust source patches (main dust fetch length). To ensure accurate estimation of dust emission fluxes over apparently homogeneous erosive surfaces, it is important to take measurements at a height above the dust blending height. This will ensure that the measurements are taken in a constant dust flux layer where dust fluxes exhibit a more spatially uniform behavior. At a landscape scale (about 1 km), when evaluating dust emission flux from a specific dust source patch, measurements should be taken within the plume emanating from the dust source patch and above the internal dust blending height associated to this patch.

Data Availability Statement

Data are available in the Zenodo data repository at https://doi.org/10.5281/zenodo.10818591 (Dupont et al., 2024).

Acknowledgments

We acknowledge the European Research Council under the Horizon 2020 research and innovation programme through the ERC Consolidator Grant FRAGMENT (Grant agreement no 773051), and the AXA Research Fund through the AXA Chair on Sand and Dust Storms at BSC for financial support of the field campaigns in Iceland and Jordan. S. Dupont acknowledge the financial support of the Department Agroecosystem of INRAE. K. Kandler and K. Schepanski are funded by the Deutsche Forschungsgemeinschaft (DFG, German Research Foundation)—416816480; 417012665. For the Icelandic campaign, we thank the staff from the ranger station at Dreki as well as the wardens of the Dreki campsite and the Dreki mountain rescue service for their valuable support and advice. We also thank Vilhjalmur Vernharðsson and his crew from Fjalladýrð for their permanent logistic help. Without all of them, the measurement campaign would not have been successfully feasible. For the Jordanian campaign, we acknowledge efforts by the staff at Wadi Rum Protected Area, Aqaba Special Economic Zone Authority, and Directorate of Environmental Monitoring and Assessment at Ministry of Environment. We also thank the Helmholtz Association's Initiative and Networking Fund (Grant agreement no VH-NG-1533) for financial support of the field campaigns in Iceland and Jordan.

References

Butler, H., Hogarth, W., & McTainsh, G. (1996). A source-based model for describing dust concentrations during wind erosion events: An initial study. *Environmental Software*, *11*(1–3), 45–52. https://doi.org/10.1016/s0266-9838(96)00036-6

Butler, H. J., McTainsh, G. H., Hogarth, W. L., & Leys, J. F. (2005). Kinky profiles: Effects of soil surface heating upon vertical dust concentration profiles in the channel country of western Queensland, Australia. *Journal of Geophysical Research*, *110*(F4), F04025. https://doi.org/10.1029/2004jf000272

Dupont, S. (2020). Scaling of dust flux with friction velocity: Time resolution effects. *Journal of Geophysical Research*, *125*(1), e2019JD031192. https://doi.org/10.1029/2019jd031192

Dupont, S. (2022). On the influence of thermal stratification on emitted dust flux. *Journal of Geophysical Research*, *127*(20), e2022JD037364. https://doi.org/10.1029/2022jd037364

Dupont, S., Klose, M., Irvine, M., González-Flórez, C., Alastuey, A., Bonnefond, J.-M., et al. (2024). Data presented in Dupont et al. 2024 "impact of dust source patchiness on the existence of a constant dust flux layer during Aeolian erosion events". [Dataset]. *Zenodo*. https://doi.org/10.5281/zenodo.10818591

Dupont, S., Rajot, J.-L., Labiadh, M., Bergametti, G., Alfaro, S. C., Bouet, C., et al. (2018). Aerodynamic parameters over an eroding bare surface: Reconciliation of the law of the wall and eddy covariance determinations. *Journal of Geophysical Research*, *123*(9), 4490–4508. https://doi.org/10.1029/2017jd027984

Dupont, S., Rajot, J.-L., Labiadh, M., Bergametti, G., Lamaud, E., Irvine, M. R., et al. (2019). Dissimilarity between dust, heat, and momentum turbulent transports during Aeolian soil erosion. *Journal of Geophysical Research*, *124*(2), 1064–1089. https://doi.org/10.1029/2018jd029048

Dupont, S., Rajot, J.-L., Lamaud, E., Bergametti, G., Labiadh, M., Khalfallah, B., et al. (2021). Comparison between eddy-covariance and flux-gradient size-resolved dust fluxes during wind erosion events. *Journal of Geophysical Research*, *126*(13), e2021JD034735. https://doi.org/10.1029/2021jd034735

Fernandes, R., Dupont, S., & Lamaud, E. (2019). Investigating the role of deposition on the size distribution of near-surface dust flux during erosion events. *Aeolian Research*, *37*, 32–43. https://doi.org/10.1016/j.aeolia.2019.02.002

Fratini, G., Ciccioli, P., Febo, A., Forgione, A., & Valentini, R. (2007). Size-segregated fluxes of mineral dust from a desert area of Northern China by eddy covariance. *Atmospheric Chemistry and Physics*, *7*(11), 2839–2854. https://doi.org/10.5194/acp-7-2839-2007

Gillette, D. A., Blifford, I. H., & Fenster, C. R. (1972). Measurements of aerosol size distributions and vertical fluxes of aerosols on land subject to wind erosion. *Journal of Applied Meteorology*, *11*(6), 977–987. https://doi.org/10.1175/1520-0450(1972)011⟨0977:moasda⟩2.0.co;2

Gillette, D. A., & Passi, R. (1988). Modeling dust emission caused by wind erosion. *Journal of Geophysical Research*, *93*(D11), 14233–14242. https://doi.org/10.1029/jd093id11p14233

González-Flórez, C., Klose, M., Alastuey, A., Dupont, S., Escribano, J., Etyemezian, V., et al. (2023). Insights into the size-resolved dust emission from field measurements in the Moroccan Sahara. *Atmospheric Chemistry and Physics*, *23*(12), 7177–7212. https://doi.org/10.5194/acp-23-7177-2023

Ishizuka, M., Mikami, M., Leys, J. F., Shao, Y., Yamada, Y., & Heidenreich, S. (2014). Power law relation between size-resolved vertical dust flux and friction velocity measured in a fallow wheat field. *Aeolian Research*, *12*, 87–99. https://doi.org/10.1016/j.aeolia.2013.11.002

Kljun, N., Calanca, P., Rotach, M. W., & Schmid, H. P. (2015). A simple two-dimensional parameterisation for Flux Footprint Prediction (FFP). *Geoscientific Model Development*, *8*(11), 3695–3713. https://doi.org/10.5194/gmd-8-3695-2015

Monin, A. S., & Obukhov, A. M. F. (1954). Basic laws of turbulent mixing in the surface layer of the atmosphere. *Tr. Akad. Nauk SSSR Geophiz.*, *24*(151), 163–187.

Raupach, M. R., Antonia, R. A., & Rajagopalan, S. (1991). Rough-wall turbulent boundary layers. *Applied Mechanics Reviews*, *44*(1), 1–25. https://doi.org/10.1115/1.3119492

Tennekes, H. (1973). The logarithmic wind profile. *Journal of the Atmospheric Sciences*, *30*(2), 234–238. https://doi.org/10.1175/1520-0469(1973)030⟨0234:tlwp⟩2.0.co;2

Wyngaard, J. C. (1990). Scalar fluxes in the planetary boundary layer? Theory, modeling, and measurement. *Boundary-Layer Meteorology*, *50*(1–4), 49–75. https://doi.org/10.1007/bf00120518

Wyngaard, J. C., & Brost, R. A. (1984). Top-down and bottom-up diffusion of a scalar in the convective boundary layer. *Journal of the Atmospheric Sciences*, *41*(1), 102–112. https://doi.org/10.1175/1520-0469(1984)041⟨0102:tdabud⟩2.0.co;2